Particle Annihilation in Cold Dark Matter Micropancakes

Craig J. Hogan
Astronomy and Physics Departments, University of Washington, Seattle, Washington 98195-1580

Cold primordial particle dark matter forms with a distribution in six-dimensional phase space closely approximating a three-dimensional sheet. Folds in the mapping of this sheet onto configuration space create ubiquitous sheetlike caustics ("micropancakes"). A typical WIMP dark matter halo has many micropancakes, each with a scale comparable to the halo itself, a width about 10^{-8} of the halo size and a typical maximum density up to about 10^4 times the halo mean. It is suggested here that the total annihilation rate of dark matter particles is dominated by particles close to these micropancakes, so radiation is emitted predominantly from highly contorted two-dimensional surfaces rather than a filled volume. The total annihilation rate of particles is about a factor of 5 higher than predicted from N-body simulations, which cannot resolve these features. Micropancakes also produce sharp line discontinuities in the surface brightness of annihilation radiation.

I. ANNIHILATING COLD DARK MATTER

Many candidates for particle dark matter separate out of the early expansion symmetrically, with equal numbers of particles and antiparticles that slowly annihilate at late times. For some of the most plausible weakly interacting massive particle ("WIMP" [1–3]) candidates, such as neutralinos, these annihilations produce GeV to TeV photons and other observable energetic species at a rate which is potentially observable and can be used to constrain the particle parameters [4–15]. Annihilations may be a source of high energy photons already seen in *EGRET* data, including diffuse emission (e.g. Ref. [16]), as well as emission from the center of the Galaxy [17] and unresolved "discrete sources" [18]. Gamma ray backgrounds will be studied with better sensitivity and resolution with future experiments such as *GLAST* [19] and *VERITAS* [20].

The physics of the annihilation is straightforward to calculate within the framework of any given particle candidate [2,3], but because the annihilation rate is proportional to the square of the particle density n, the calculated rate of annihilations and their spatial distribution depend on astrophysically complex features of the detailed small-scale spatial distribution of the dark matter particles. The best calculations [15] use high-resolution N-body simulations to compute the dark matter distribution including clumpy relic substructure within halos [21,22] and high density central cusps [21–25], both of which are important to the annihilation rate and the expected appearance of the radiation on the sky. This paper suggests that even smaller predicted structures, sheetlike caustics or "micropancakes", which are not included in even the best N-body calculations, significantly increase the total annihilation rate and change the predicted fine-scale spatial distribution of emission.

II. MICROPANCAKES OF COLD DARK MATTER

CDM particles are created in the early universe as a smooth Hubble flow ($\vec{v} = H\vec{r}$) with small random velocities, and therefore occupy a sheet in phase space that is thin in three of the six phase space dimensions. Liouville's theorem guarantees that during subsequent collisionless evolution, the fine grained distribution always remains one continuous unbroken thin sheet, although it wraps up in a complicated pattern once nonlinear structures form. In the emptiest parts of intergalactic space today, the sheet still passes through each point in space only once; in collapsed systems, it passes many times, so that the velocity distribution at any point in a CDM halo better approximates a discrete rather than a continuous function [27].

The wrapping of the phase space sheet (see figures 1 and 2) creates singularities in the mapping from phase space onto configuration space [28,29]. The most generic are the two-dimensional sheetlike "fold catastrophes", although there are also higher order catastrophes at their intersections. We will call these two-dimensional caustics "micropancakes" (in contrast to the much larger Zeldovich pancakes or "*blini*" [30] which form in hot-dark-matter cosmologies). They occur at the surfaces in space where the number of phase sheets changes.

The density n of particles near a micropancake follows the universal profile of a fold catastrophe; it formally diverges on one side according to the universal scaling $n \propto \delta\ell^{-1/2}$ where $\delta\ell$ is the normal distance to the micropancake, and drops discontinuously on the other side as the number of projected sheets drops by two. The physical width of the density discontinuity is limited only by the fine-grained width of the phase sheet— which is in turn fixed by the primordial particle velocity dispersion of the dark matter.

Physically, micropancakes form at the turning points of the particle flow in the frame moving locally with the particles. They appear in exactly symmetric (spherical, cylindrical or planar) solutions of halos and voids (e. g. [31–33]), but micropancakes are not an artifact of any symmetry; they are a robust and generic prediction of the CDM scenario. An isolated spherically symmetric halo forms new micropancakes like tree rings, one per "year" (or gravitational crossing time); for typical CDM halos with a rich substructure, the older substructures themselves also contain a highly wrapped structure with hundreds of folds.

Although freshly formed micropancakes are associated with the sheets and filaments defining the "cosmic web" [34], they are not the same thing; the micropancakes are pathological sites involving only a vanishing portion of the matter at very high density at any given time, whereas the cosmic web structures define the organization of a large fraction of the material. A fairly accurate visual metaphor is the pattern of sunlight in a swimming pool: most of the light is cast into a weblike pattern, but only a small fraction into bright caustic lines.

Indeed, the main reason why this rich structure has received rather little attention in the literature is that it has few observable effects on astrophysical phenomenology. The micropancakes contain only a small amount of mass at high density, and have relatively little effect on the smooth gravitational potential or on the dynamics of observable stars and gas [26] (but see [35]). For the same reason, they do not appear in N-body simulations. However, the preservation of the coherent cold phase space streams which necessarily give rise to the micropancakes at their turning points has been demonstrated in simulations (for example, by constructing Poincarè projections showing distribution of particles in isolated islands in phase space [26]), so we know that micropancakes are indeed predicted by the physical CDM model. In principle, a detailed study of these could be used to estimate many properties of the micropancakes more accurately than the rough estimates presented here.

In spite of their negligible overall dynamical effects, there are a few phenomena where the pathological properties of micropancakes may be observable. These phenomena are of particular interest as a probe of the nature of the dark matter, since the finite width of the caustics preserves information about the primordial fine-grained phase density.

III. MICROPANCAKES IN HALOS

Many real astrophysical systems display something like phase-wrapping folds [29], but particle CDM (and in particular WIMP) micropancakes are unusually good approximations to ideal catastrophes over an exceptionally large dynamic range. Because the particles form with a very high microscopic phase density, their caustics create a local physical density enhancement of many orders of magnitude over the halo mean.

Suppose a candidate of mass $m_X \approx 1$GeV separates from the thermal cosmological plasma at a temperature of $T_{sep} \approx 0.1$ GeV (typical for Lee-Weinberg weakly interacting dark matter). The fine-grained primordial phase space density $Q_P \equiv \rho\sigma_X^{-3}$ is determined by the physics of the dark matter: the momentum distribution of the dark matter particles is fixed at T_{sep}. Normalized to the present density of dark matter $\rho_0 \approx 0.3\rho_{crit}$,

$$Q_P \approx 10^{36}\frac{\rho_0}{c^3}\left(\frac{m_X}{\mathrm{GeV}}\right)^{3/2}\left(\frac{T_{sep}}{0.1\mathrm{GeV}}\right)^{3/2}. \tag{1}$$

This phase density is conserved during adiabatic expansion, so the velocity dispersion σ_X at a redshift z, in units with $c = 1$, is about

$$\sigma_X(z) \approx 10^{-11.5}(m_X/\mathrm{GeV})^{-1/2}(T_{sep}/0.1\mathrm{GeV})^{-1/2}[(1+z)/3] \tag{2}$$

in the absence of any clustering. For collisionless particles, the fine-grained density of the phase sheet retains the primordial value Q_P even after nonlinear collapse [36,37]. For standard WIMPs, the collisionless approximation is very good; gravitational two-body scattering is negligible, and other processes such as annihilation and scattering involve weak interactions that are negligible after T_{sep}.

The evolution of the phase sheet in the nonlinear CDM hierarchy is very complex; for this discussion, we only estimate the properties in smooth halos characterized by a single density ρ_{halo} and velocity dispersion σ_{halo}. We assume that there are few hard scattering centers, so that the main mixing of the phase sheet is coarse-grained violent relaxation in halos on each scale of the hierarchy. There is then only one length scale ℓ_{halo} in each halo and most of the orbits retain much of their coherence (as seen in both simulations and in observations of Galactic stellar moving groups [38].) We assume that the large dimensions of the folds is mostly comparable with the scale of the halo. The number of folds N grows only linearly (not exponentially) with time (although a chaotic system could lead to a more rapid phase space mixing that would tend to erase micropancakes; see [39]). These estimates can be applied to a hierarchy by regarding subhalos as separate bound systems.

Suppose a halo has N folds of the sheet which add up to the total spatial density ρ_{halo}; then from mass conservation, the space density of each single sheet is about ρ_{halo}/N, times factors of the order of unity depending on the halo profile and geometry. (This description is only adequate for real halos over a limited dynamic range in radius. For example, the outermost regions of a halo still forming out of the expansion would have $N = 1$, the density and radius of the outermost caustic corresponding to the first turnaround of particle orbits; both N and ρ_{halo} increase at smaller radii.) Conservation of local fine-grained phase density then allows us to estimate from this density the typical fine-grained velocity dispersion σ_{Xhalo} in the wrapped up sheet (far away from the caustics),

$$\frac{\sigma_{Xhalo}}{\sigma_{halo}} \approx \left(\frac{\bar{Q}}{Q_P}\right)^{1/3} N^{-1/3} \tag{3}$$

where $\bar{Q} \equiv \rho_{halo}/\sigma_{halo}^3$ denotes the mean coarse-grained phase space density of the halo.

The fine-grained nonlinear evolution of the phase sheet can be described using action-angle variables [40,41]. Although exact results have only been derived in symmetric situations, we can again roughly estimate the properties of the caustics in the general case. The finite minimum spatial width ℓ_{min} of the micropancakes can be estimated by noting that the turning points of the orbits for particles in one sheet have a spatial dispersion about the mean location of the sheet proportional to the dispersion in velocity integrated over an orbital time, hence

$$\frac{\ell_{min}}{\ell_{halo}} \approx \frac{\sigma_{Xhalo}}{\sigma_{halo}} \approx \left(\frac{\bar{Q}}{Q_P}\right)^{1/3} N^{-1/3} \approx 10^{-8} N^{-1/3}. \tag{4}$$

Near a micropancake, the velocity dispersion in the normal direction increases to a saturated value σ_{sat} depending on Q_P and the curvature of the sheet in phase space. For folds curving on the halo scale of length and velocity, with the two large dimensions both close to the halo size, the dispersion saturates at a value

$$\sigma_{sat}/\sigma_{halo} \approx (\ell_{min}/\ell_{halo})^{1/2} \approx (\sigma_{Xhalo}/\sigma_{halo})^{1/2}, \tag{5}$$

times numerical factors depending on the geometry of the fold. The typical maximum saturated density ρ_{max} is then approximately given by $Q_P \sigma_{sat} \sigma_{Xhalo}^2$, or

$$\frac{\rho_{max}}{\rho_{halo}} \approx \left(\frac{\ell_{min}}{\ell_{halo}}\right)^{-1/2} N^{-1} \approx \left(\frac{Q_P}{\bar{Q}}\right)^{1/6} N^{-5/6} \approx 10^4 N^{-5/6}. \tag{6}$$

The value of $\bar{Q}$ for real halos varies by over nine orders of magnitude, from dwarf spheroidals to galaxy clusters [37]; the numerical values here estimate $\bar{Q}$ for "typical" CDM halos using $(\bar{Q}/Q_P)^{1/3} \approx (\sigma_X(z_{coll})/\sigma_{halo})$ at a collapse redshift $z_{coll} \approx 10$, and a velocity dispersion $\sigma_{halo} \approx 10^{-3}$. The number of folds is of the order of the dynamical age of the halo in units of the gravitational crossing time, $N \approx 1$ to 100 for typical halos. The powers of N in these estimates change if we make different assumptions about the micropancake geometry; such effects can lead to factors of ≈ 2 difference in the annihilation rate estimates below.

The density enhancement near the micropancakes within each halo or subhalo is around a factor of 10^4, although the total contrast is less for old halos or dense central regions with many folds. The angular size of the sharp edges is less than 10^{-8} of the halo size, and the dynamic range, the ratio of size to separation, is about $10^{-8} N^{2/3} \approx 10^{-6}$ (hence the name, "micropancakes").

IV. ANNIHILATION RATE WITH MICROPANCAKES

One possible technique for measuring the properties of these tiny caustics is "micopancake microlensing" [28]. The projection of micropancakes onto the plane of the sky leads to line discontinuities in surface density which produce universal signatures in the gravitational lensing of background stars or other sources: images of very distant stars occasionally suddenly appear or disappear, and extended sources occasionally display mirror-reflected images about a sharp line discontinuity. Detection of these exotic effects is however well beyond current observational capability.

Here we estimate another, possibly more easily observable consequence of micropancakes: their influence on dark matter particle annihilation. Although each particle spends only a small amount of time in micropancakes, the density is so high that most of the annihilations take place there. The micropancakes therefore alter the annihilation rate by a large factor.

Micropancakes occur on such a small scale that they are not resolved in CDM simulations (this is even true of the largest, "freshest" pancakes, because they occur in those relatively underdense parts of space where CDM codes are designed for speed to have the poorest resolution). Because of this, the statistical properties of their spatial distribution are poorly characterized compared to the other predictions of CDM. We know that orbital phase mixing eventually homogenizes phase space; however, the estimate above suggests that it takes a very large number of orbits (perhaps as many as $N \approx 10^{4\times 6/5} \approx 10^5$ for smooth halos) to mix thoroughly enough to destroy the micropancakes. Until this happens, micropancakes are ubiquitous and a typical particle will participate in one at a turning point about every orbit. This is enough information to estimate the magnitude of the effect on annihilation rates.

Suppose that the probability of annihilation per particle per time is $n\sigma v$, where n is the number density of (anti)particles and σv is some constant determined by the physics of the dark matter (e.g., [2]). Normalizing to unit size, virial velocity and orbital time for the local halo of density n_0, close to the pancake the universal fold catastrophe profile gives $n \approx n_0 \delta\ell^{-1/2}$ within distance $\delta\ell$ of a micropancake. Each particle enters and leaves the pancake at a turning point of its orbit, so its velocity relative to the frame of the pancake is $\delta\dot{\ell} \approx \delta\ell^{1/2}$; each particle trajectory in this frame is $\delta\ell(t) \approx t^2$; and the integrated annihilation probability is therefore

$$\int dtn\sigma v \approx n_0 \sigma v \int dt/t. \tag{7}$$

The integrated annihilation probability is therefore logarithmically divergent as $t \to 0$ or $\delta\ell \to 0$, the moment when the particle passes through the micropancake. Since each particle passes through one of these caustics every orbit, this means that the overall annihilation integral is dominated by the particles close to the pancakes. An equivalent formulation is to discuss the probability distribution of n, which has a power-law tail due to matter near micropancakes, $dP(n)/dn \propto n^{-2}$. The annihilation rate is then $\int dnn(dP(n)/dn) \propto \int d\ln n$, again displaying the high-n logarithmic divergence.

This leads to the first main conclusion,

- The annihilation radiation comes predominantly from contorted two-dimensional surfaces, rather than from a volume-filling source.

An important corollary of this is that:

- The mean annihilation rate is higher than one would estimate from N-body studies of clumping— even those of the highest resolution— by a significant factor.

The exact value of this factor is not known but we can estimate roughly from the maximum density contrast of the micropancakes, estimated above. For each virialized halo or subhalo, the total rate is higher than one would guess from the mean local density by a factor of $\ln(10^4) - (5/6)\ln N \approx 9 - (5/6)\ln N$, about a factor of 5. The bulk of the integral comes far below the resolution limit of simulations, from the small fraction of particles closest to the micropancakes. The argument holds for all systems and subsystems within a halo, or for different radii within a halo, although the $\ln N$ reduction reflects a smaller enhancement factor in higher density regions (as the density enhancement in pancakes is diluted by wrapping). In the absence of micropancakes, the bulk of annihilations are predicted to occur in a small fraction of mass in the dense parts of halos; this argument indicates that within those dense parts, the micropancakes dominate.

V. LINE DISCONTINUITIES IN BRIGHTNESS

If the CDM annihilations produce direct gamma ray emission (as opposed to indirect emission via e^+e^-), the radiating surfaces may be imaged. For radiation in a monochromatic line, a "velocity cube" map (two sky directions and a redshift) would show emission concentrated in two-dimensional sheets, giving a direct three-dimensional image of the micropancakes. However, if the annihilations produce continuum radiation or if the velocity resolution is insufficient to separate the sheets, we should calculate instead the mean surface brightness of the annihilation radiation. This is given by the line-of-sight integral

$$I = \int dzn^2(z)\sigma v. \tag{8}$$

Consider now the surface brightness near the line in the sky where a micropancake lies normal to the plane of the sky, and is seen edge-on. Choose coordinates which place the line at $\ell = 0$ in the plane of the sky, and at $z = 0$

along the line of sight. The line-of-sight distance to the sheet at a projected distance ℓ_p is given (again, in locally appropriate units) by $z = \ell_p^{1/2}$ — another fold catastrophe, this time of the mapping of the 2D micropancake sheet onto the sky (rather than the 3D phase space sheet onto 3D configuration space). The density of material is thus $n = (\ell_p - z^2)^{-1/2}$, and the projected surface brightness at $\ell_p \geq 0$ becomes

$$I \approx 2n_0^2 \sigma v \int_0^{\ell_p^{1/2}} \frac{dz}{\ell_p - z^2} \approx 2n_0^2 \sigma v = \text{const}(\ell_p), \tag{9}$$

while of course there is no flux at $\ell_p < 0$. Thus, the folded micropancakes create abrupt discontinuities in surface brightness:

- The sky projection of direct emission from a halo of annihilating particles is laced by sharp line discontinuties in brightness, the number N of them approximately equal to the dynamical age.

For WIMP dark matter, detailed study of the annihilation radiation background may thus contain information complementary to that obtainable by direct detection experiments. However, the experimental challenges are daunting. Verifying the existence of the discontinuities (as opposed to resolving them) requires enough resolution to separate the projected lines. For the most part the lines are closer than N^{-1} times the projected separation scale of galaxies at the Hubble length, on the order of arcseconds or smaller (although a small fraction of the light comes from much larger local halos, including some long caustic threads from our own Galaxy stretching across the sky). The amplitude or fractional contrast of each line discontinuity is small, of the order of N^{-1}; and as shown by the N-body studies, most of the flux is coming from dynamically older, compact substructures within halos (which have large $N \geq 10^2$).

Measuring the width of the discontinuity, as would be necessary to actually measure $\bar{Q}$ directly, is even more challenging. As discussed above, it is set by the intrinsic width of the CDM phase sheet; for WIMP dark matter, this corresponds to an angle of about 10^{-8} of the angular size of the halo under study. Such a small-scale, low contrast angular structure will not be resolved by currently planned GeV-to-TeV background mapping experiments.

ACKNOWLEDGMENTS

I am grateful for conversations with R. Blandford, A. Helmi, M. Kamionkowski, B. Moore, T. Quinn, S. White, and the referee. This work was supported at the University of Washington by NSF grant AST-9617036.

VI. REFERENCES

[1] B. W. Lee, & S. Weinberg, Phys. Rev. Lett. **39**, 165 (1977)
[2] G. Jungman, M. Kamionkowsky, & K. Griest, Phys. Rep. **267**, 195 (1996).
[3] L. Bergström, Nucl. Phys. B – Proc. Suppl. **70**, 31 (1999).
[4] J. E. Gunn, B. W. Lee, I. Lerche, D. N. Schramm, & G. Steigman, Astrophys. J. **223**, 1015 (1978).
[5] F. W. Stecker, Astrophys. J. **223**, 1032 (1978).
[6] J. Silk, & M. Srednicki, Phys. Rev. Lett. **53**, 624 (1984).
[7] M. S. Turner, Phys. Rev. D **34**, 061921 (1986).
[8] J. Silk, & H. Bloemen, Astrophys. J. **313**, L47 (1987).
[9] A. Bouquet, P. Salati, J. Silk, Phys. Rev. D **40**, 103168 (1989).
[10] G. Lake, Nature **346**, 39 (1990).
[11] L. Bergström, J. Edsjö, P. Gondolo, Phys. Rev. D **58**, 103519 (1998).
[12] E. A. Baltz, & J. Edsjö, Phys. Rev. D **59**, 023511 (1999).
[13] P. Gondolo, & J. Silk, Phys. Rev. Lett. **83**, 1719 (1999).
[14] E. A. Baltz, C. Briot, P. Salati, R. Taillet, & J. Silk, Phys. Rev. D **61**, 023514 (2000).
[15] C. Calcáneo–Roldán & B. Moore, Phys. Rev. D **62**, 123005 (2000)
[16] D. D. Dixon, D. H. Hartman, E. D. Kolaczyk, J. Samimi, New Astron. **3**, 539 (1998).

[17] H. A. Mayer-Hasselwander et al., Astron. Astrophys. **335** 161 (1998).
[18] R.C. Hartman et al., Astrophys. J. Supp. **123**, 79 (1999).
[19] see http://glast.gsfc.nasa.gov/
[20] see http://veritas.sao.arizona.edu
[21] S. Ghigna, B. Moore, F. Governato, G. Lake, T. Quinn, & J. Stadel, Mon. Not. R. Astron. Soc. **300**, 146 (1998).
[22] B. Moore, astro-ph/0103100 (2001).
[23] R. G. Carlberg, Astrophys. J. **433**, 468 (1994).
[24] J. F. Navarro, C. S. Frenk, & S. D. M. White, Astrophys. J. **462**, 563 (1996).
[25] B. Moore, F. Governato, J. Stadel, T. Quinn & G. Lake, Astrophys. J. Lett. **499**, L5 (1998)
[26] B. Moore, submitted to idm2000, World Scientific, astro-ph/0103094 (2001)
[27] P. Sikivie, Phys. Lett. B, **432**, 139 (1998)
[28] C. J. Hogan, Astrophys. J. **527**, 42 (1999)
[29] S. Tremaine, Mon. Not. R. astr. Soc., **307**, 877 (1999)
[30] Ya. B. Zeldovich 1970, Astrofizika, **6**, 319 (English transl. in Astron. Astrophys, **5**, 84 [1970])
[31] J. A. Fillmore & P. Goldreich, ApJ, **281**, 1 (1984)
[32] J. A. Fillmore & P. Goldreich, ApJ **281**, 9 (1984)
[33] E. Bertschinger ApJS, **58**, 39 (1985)
[34] J. R. Bond, L. Kofman, & D. Pogosyan, Nature **380**, 603 (1996)
[35] P. Sikivie, Phys. Rev. D **60**, 063501 (1999)
[36] C. J. Hogan, & J. J. Dalcanton, Phys. Rev. D, **62**, 063511 (2000)
[37] J. J. Dalcanton & C. J. Hogan, ApJ, submitted, astro-ph/0004381 (2001)
[38] A. Helmi, S. D. M. White, P. T. de Zeeuw, & H. Zhao, Nature **402**, 53 (1999)
[39] J. Goodman, J. C. Heggie, & P. Hut, ApJ, **415**, 715 (1993)
[40] A. Helmi, "The Formation of the Galactic Halo," Ph. D. Thesis, Leiden (2000)
[41] A. Helmi & S. D. M. White, Mon. Not. R. Astron. Soc. **307**, 495 (1999)

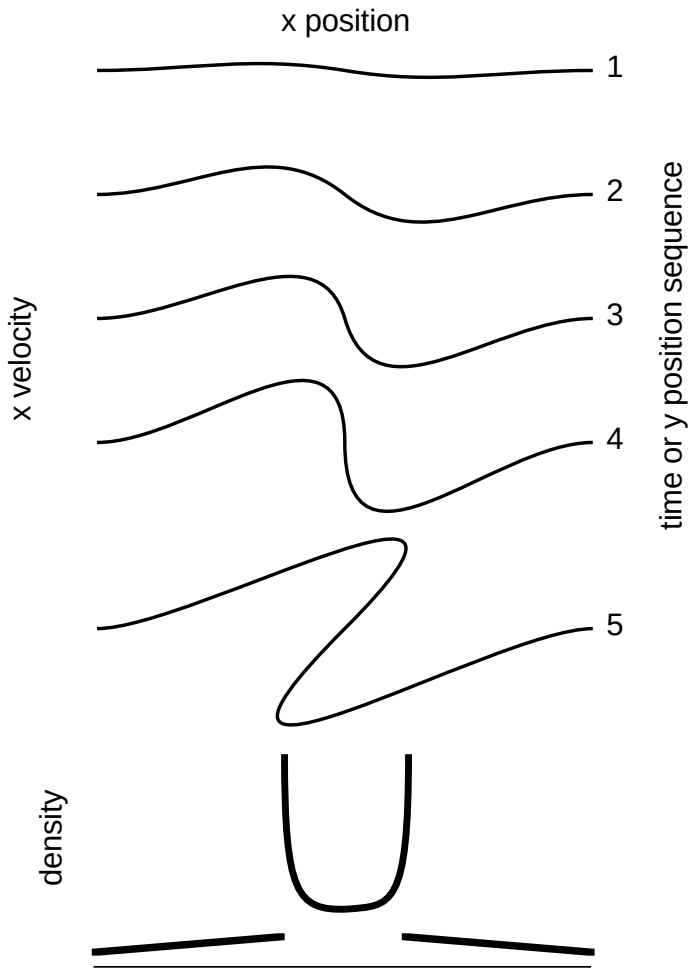

FIG. 1. Generic behavior of CDM sheet in phase space during formation of a single fold catastrophe. Curves show two dimensions of six-dimensional phase space, say x and the x component of velocity, v_x. The sequence of curves can be regarded as a time sequence as a fold forms, or as a x, v_x cross section at various spatial positions y. The fold caustics formed in step 5 project formally infinite density in configuration space; a density profile cut along x is shown. The actual width and maximum density in the "singularity" are limited by the intrinsic (primordial) width of the CDM phase sheet.

FIG. 2. Sketch of the formation of micropancakes, showing the topology of the singularities in configuration space. The first nonlinear collapse (with 2D phase space shown in figure 1) forms a small ravioli-like structure of two micropancakes (fold singularities) joined around the edges (terminating in cusp singularities), which then grows. If the structure is bound, a second ravioli forms inside the first (now a calzone) after another orbit, and so on. In general a violently-relaxed CDM halo (or subhalo) is threaded with many micropancakes at turning points of orbital streams, showing some coherence but with no particular symmetry. This microstructure appears within each satellite of a CDM galaxy halo.